MICROWAVE AND SOLID STATE ASSISTED SYNTHESIS OF LSMO: $NiFe_2O_4$ NANOCOMPOSITES AND COMPARATIVE STUDY OF ITS MICROSTRUCTURAL AND MAGNETIC PROPERTIES

A THESIS SUBMITTED IN PARTIAL FULFILLMENT
OF THE REQUIREMENTS FOR THE DEGREE OF

Bachelor of Technology
in
Ceramic Engineering

By
RAHUL MOHANTY

Department of Ceramic Engineering
National Institute of Technology
Rourkela
2011

MICROWAVE AND SOLID STATE ASSISTED SYNTHESIS OF LSMO: $NiFe_2O_4$ NANOCOMPOSITES AND COMPARATIVE STUDY OF ITS MICROSTRUCTURAL AND MAGNETIC PROPERTIES

A THESIS SUBMITTED IN PARTIAL FULFILLMENT
OF THE REQUIREMENTS FOR THE DEGREE OF

Bachelor of Technology
in
Ceramic Engineering

By
RAHUL MOHANTY

Under the Guidance of
Prof Bibhuti B. Nayak

Department of Ceramic Engineering
National Institute of Technology
Rourkela
2011

National Institute of Technology

Rourkela

CERTIFICATE

This is to certify that this thesis entitled, "MICROWAVE AND SOLID STATE ASSISTED SYNTHESIS OF LSMO: $NiFe_2O_4$ NANOCOMPOSITES AND COMPARATIVE STUDY OF ITS MICROSTRUCTURAL AND MAGNETIC PROPERTIES" submitted by Mr. RAHUL MOHANTY in partial fulfillments for the requirements for the award of Bachelor of Technology Degree in Ceramic Engineering at National Institute of Technology, Rourkela is an authentic work carried out by him under my guidance.

To the best of my knowledge, the matter embodied in the thesis has not been submitted to any other University / Institute for the award of any Degree or Diploma.

Date:

Prof Bibhuti B Nayak
Associate Professor
Department of Ceramic Engineering,
National Institute of Technology,
Rourkela- 769 008

ACKNOWLEDGEMENTS

I owe a great many thanks to a great many people who helped and supported me for the completion of this project effectively and moreover in time.

First, I express my deepest thanks to Prof. Bibhuti B. Nayak, Department of Ceramic Engineering, National Institute of Technology Rourkela for giving me an opportunity to carry out this project under his supervision. He has been very kind and patient while suggesting me the outlines of this project and has clarified all my doubts whenever I approached him. I thank him for his overall support.

My deep sense of gratitude to M-tech and PhD Scholars, Subrat Bhai, Nadiya Bhai, Geeta dee, Sanjay Bhai, Sarat Bhai, Bhabani Bhai, Abhishek Bhai, Ganesh Bhai and others who were there to give me company in the lab and helped me with best possible ways.

I m equally thankful to Prof. Pratihar for helping me out with DSC-TG of the samples, and I am much obliged for that. Prof Mazumder, Prof Sarkar, Prof Sarkar, Prof. Choudhury, Prof Pal, Prof Bhattacharya and last but not the least our department HOD, my faculty advisor, Prof Bera have imparted me knowledge and wisdom and have borne me for so many days. Thank you, Sirs. Words are not enough to acknowledge your contribution in my life.

Mr. Rajesh Pattnaik, Department of Metallurgy, for helping me out with the SEM analysis. I'm indebted to him for that.

I would also like to say "Thank You" to all my batch mates (Dept. of Ceramic), National Institute of Technology Rourkela for their constant moral support and motivation.

Finally, thanks and appreciation to everyone else involved in this project with me at National Institute of Technology Rourkela.

5th May 2011 ***Rahul Mohanty***

CONTENTS

Abstract

This project work is an appraisement of the effect of the synthesis route followed for the synthesis of LSMO: NFO composites, of different ratios.

LSMO and NFO individually have variety of applications, because of LSMO's CMR behavior and NFO acts as soft ferrites with very low retentivity. But on varying the temperature of the LSMO the change in structure as well as change in magnetic behavior is observed. The double exchange process, which mediates electrical and magnetic transitions, depends on external factors and is highly susceptible to processing conditions and the chemical composition. Whereas NFO has its application in various daily life used equipments.

Our objectives in the present work include the microwave synthesis of LSMO: NFO composite through in-situ and solid-solid route, and to study the structural, microstructural and magnetic hysteresis loop.

In the first part of the work relates to sample synthesis by in-situ route and its characterization. It was studied from DSC-TG that the calcine temperature of the composites is around 800-1000 ^{o}C. The SEM images show the compactness of the in-situ prepared samples and the crack propagation is mostly through the grain boundary. It was revealed that the NFO phase lies mostly around edge of the grain boundary or at the junction of grains. The particle size of NFO is much smaller than LSMO.

The second part of my work mostly deals with the study of magnetic hysteresis loop of both in-situ route and solid route synthesized samples. It was revealed at the room temperature there is an increase in the distortion in the hysteresis loop with the increase in percentage of LSMO in the composite. This helps us to synthesize sample as per the requirement for an application.

Keywords: LSMO (La–Sr–Mn–O) and NFO ($NiFe_2O_4$); SEM-scanning electron microscope.

List of Figures

List of Tables

Chapter 1

INTRODUCTION

1.1 Introduction

Manganites like La–Ca–Mn–O (LCMO), and La–Sr–Mn–O (LSMO), have been studied extensively in the recent past as they exhibit simultaneous magnetic and electrical transitions in certain composition ranges. They undergo a paramagnetic, semi conducting to ferromagnetic, metallic transition on cooling which is accompanied by a large conductivity enhancement in the presence of an external magnetic field —negative magneto resistance [1]**.**

The decrease in magneto-resistance in these oxides becomes extremely large, near the transition temperature, a phenomenon of great interest to information storage applications. In the presence of relatively low fields the magnitude of magneto resistance increases with , grain size reduction or substitution doping [2].

In the present work, two methods were followed to prepare composites of LSMO and NFO. The techniques are in-situ route and solid state route. The in-situ process uses microwave assisted refluxing. This technique has an inherent advantage of uniformly mixing the precipitates formed after co-precipitation method. The precipitates will also have a similar grain size distribution as they will be subjected to identical processing conditions [3].

The interesting aspect of these nanocomposites is that above the transition temperatures corresponding to LSMO/LCMO phase, the nanocomposite will be electrically insulating but magnetic due to the presence of ferrite and similarly at room temperature, they will show magnetic behavior(LSMO doesn't shows any magnetic property at room temperature). Below the transition temperatures of LSMO/LCMO the composite will be conducting and also magnetic with a colossal MR behavior. This temperature dependent behavior makes it attractive for innovative applications in magnetic information storage [4].

1.2 Outline of the report

The introduction for the proposed project is given in this chapter. Then the next chapter is all about the literature that was needed to be done for getting the assistance needed for the project. The third chapter is mostly about the experimental and synthesis techniques used to process the required samples. The result and discussion of the characterized samples were given in the fourth chapter and the conclusion prior to the result analysis is provided in the final chapter; which will help with the future work.

Chapter 2

LITERATURE REVIEW

2.1 Structure and properties of manganites

There has been a lot of research and study in Colossal Magnetoresistancce (CMR) effects in rare-earth manganite perovskite with general formula $La_{1-x}A_xMnO_3$ (A = Ba, Sr, Pb and Ca) due to their potential technology application).The pervoskite structure consists of on a lattice of oxygen octahedral with Mn ion in their centre. Therefore there is oxygen between every two manganese. A/B cations are placed in between the octahedra. Most studies has been done on $La_{1-x}Ca_xMnO_3$ and $La_{1-x}Sr_xMnO_3$. The oxygen has a full outer shell (2p) being in a O^{2-} state. The above compounds are rich with $Mn^{3+}$and doping of divalent atoms introduces mixture valence of Mn^{3+} and Mn^{4+} ions plays a major role in Double Exchange (DE) ferromagnetic interaction coupled with metallic resistivity. Double exchange effect is an exchange of electrons from neighboring Mn^{3+} to Mn^{4+} ions through oxygen when their core spin are parallel [5]. Moritomo *et al* [6] showed that the tridimensional $La_{1-x}Sr_xMnO_3$ does not present a metal to insulator transition being metallic above Tc. The single layered version of it, $La_{1-x}Sr_{1+x}MnO_4$ is neither metallic nor ferromagnetic while the double layered $La_{1-x}Sr_{1+}2xMn2O_7$ shows an intermediate behavior: it presents a metal to insulator transition. However, it has been claimed that an additional mechanism, Jahn-Teller distortion (JT) could be responsible for the transport properties.

The Magnetoresistance (MR) percentage of MR defined as:

$[(R_H\text{-}Ro)/Ro]*100$

Where R_H is the resistance in the present of magnetic field and Ro is the resistance at zero fields.

In general, CMR effects of polycrystalline ceramic bulk exhibit two classes of Magnetoresistance (MR): intrinsic and extrinsic MR. The latter is observed in manganites and is due to the intergrain effect where higher MR could be observed over a wider temperature range below Tc and is characteristic of a Low-Field MR (LFMR), Higher MR was observed well below Tc where MR value increased monotonically with the decrease of temperature.

2.2 Structure and properties of ferrites

Ferrites are belongs to one of the important classes of material, which found applications in high density magnetic storage, electronic anf microwave devices, telecommunication equipments magnetic fluids, magnetically guided drug delivery and gas sensors [7-12]

Ferrites are magnetic compounds which contain iron oxide (Fe2O3) as their main component [13]. Ferrite is a ferromagnetic compound i.e. magnetic moments of atoms in different sub lattices are opposed and are unequal and therefore spontaneous magnetization can randomly flip direction under the influence of temperature. They show big resistance. Ferrites are hard and brittle. They can be classified as soft and hard ferrites. Soft ferrites have low coercivity and hard have high coercivity and high remanence [14].

Most of the ferrites have a spinel structure. Spinel has formulae AB2O4.The spinel unit cell is a cubic closed pack array of 64 tetrahedral voids and 32 octahedral voids. The A and B are cations which occupy the tetrahedral and octahedral voids respectively. A is divalent and B is trivalent. There are some ferrites which have a hexagonal structure (e.g. barium ferrite).

But in this project our main concern is Ni-ferrite ($NiFe_2O_4$), which has an inverse spinel structure. The crystal structure is face centered cubic with the unit cell containing 32 oxygen ions. These oxygen ions form 64 tetrahedral and 32 octahedral sites, where 24 cations are distributed. The eight Ni2+ ions occupy eight tetrahedral sites [15, 16]

2.3 Microwave synthesis of manganite ferrite composite

Yan et al. [15] and Huang et al. [17] have studied the effect of insulating, ferromagnetic (FM) phase on the magnetotransport and magnetic behavior of La–Sr–Mn–O. They find that the presence of FM phase influences the magneto transport by magnetically coupling to the LSMO grains. The results of this work show that for $x \geq 0.05$M NF, the electrical transition is completely suppressed and the transport is dominated by a semiconducting/ insulating behavior. This is because the Mn site in LSMO is substituted by Ni and Fe which stabilize the semiconducting behavior. The MR for the 0.01M NF composite shows an increasing behavior with decreasing temperature. The MR is found to be 16% at 85K in a field of 8.5 kOe.

Nayak et al. [18] have synthesized the composite of LCMO and NF by microwave refluxing method. The in situ preparation technique results in the formation of uniformly distributed nanograined composite mixture of the two phases.

The double exchange process, which mediates electrical and magnetic transitions, depends on external factors and is highly susceptible to processing conditions and the chemical composition. In the case of pure LCMO the double exchange process is due to electron transport via Mn^{3+}–O^{2-}–Mn^{4+}. Addition of transition metal ions which substitute either the Mn^{3+} or Mn^{4+} are known to suppress the double exchange process and promote insulating, antiferromagnetic behavior. The lowering of electrical and magnetic transition temperatures coupled with an increase in absolute resistivity with the addition of NF to LCMO showed that the double exchange process in LSMO was severely affected [19].

2.4 Objectives

1. Since very little work has been reported in literature regarding the synthesis and composite of LSMO and NFO samples, the present work seeks to deal with the following:
2. Synthesis of LSMO powders using in-situ microwave synthesis route.
3. Synthesis of NFO powders using in-situ microwave synthesis route.
4. Preparation of pallets of different composition of NFO and LSMO (80LSMO:20NFO, 60LSMO:40NFO, 50LSMO:50NFO), with two different routes in-situ and solid route.
5. Study of the effect of change in percentage of LSMO with the composition; using DSC-TG, XRD, SEM; and the variation in bulk density and apparent porosity.

Chapter 3

EXPERIMENTAL WORK

3.1 Synthesis of pure LSMO and $NiFe_2O_4$

3.1.1 Experimental Setup

Synthesis of pure nickel ferrite:-

1. Molecular calculation for weight of the salts required for a 7g batch of nickel ferrite was calculated.

Amount of salts required:-

a. Nickel chloride = 10.1415 g

b. Ferric chloride = 13.840 g

2.100ml of 1, 2 ethanediol was taken in a beaker and the above salts were added one by one with heating and stirring till the salts completely dissolve. This is solution 1.

3. A solution of KOH was prepared by dissolving 20 grams of solid KOH in 100 ml 1, 2 ethanediol. This is solution 2.

4. Solution 2 is slowly added to solution 1 to increase the pH to about 12 or 13. A gel formation will be observed.

5. The precipitate is then refluxed in a microwave oven for 60 min.

6. After refluxing the precipitate is washed to reduce the pH to 7. After this the gel is dried and ground to a fine powder.

7. The powder was calcined at a temperature of 1100 ^{o}C.

Synthesis of pure lanthanum strontium manganese oxide:-

1. Molecular calculation for weight of the salts required for a 7 g batch of lanthanum strontium manganese oxide was calculated.

Amount of salts required:-

a. Lanthanum acetate = 10.12 g

b. Strontium chloride = 2.3 g.

c. Manganese acetate = 10.756 g

2.100ml of 1, 2 ethanediol was taken in a beaker and the above salts were added one by one with heating and stirring till the salts completely dissolve. This is solution 1.

3. A solution of KOH was prepared by dissolving 20 grams of solid KOH in 100 ml of 1, 2 ethanediol. This is solution 2.

4. Solution 2 is slowly added to solution 1 to increase the pH to about 12 or 13.A gel formation will be observed.

5. The gel is then refluxed in a microwave oven for 60 min.

6. After refluxing the precipitate is washed to reduce the pH to 7.After this the precipitate is dried and ground to a fine powder.

7. The powder is calcined at a temperature of 1100 ^{o}C.

3.2 Microwave assisted in-situ synthesis of LSMO: $NiFe_2O_4$ composites

3.2.1 Experimental Setup

1. Molecular calculation for weight of the salts required for a 7 g batch of nickel ferrite was calculated.

Amount of salts required according to their composition is given below in the table.

2.100ml of 1,2 ethanediol was taken in a beaker and the above salts were added one by one with heating and stirring till the salts completely dissolve. This is solution 1.

3. A solution of KOH was prepared by dissolving 20 g of solid KOH in 100 ml of 1, 2 ethanediol. This is solution 2.

4. Solution 2 is slowly added to solution 1 to increase the pH to about 12 or 13.A gel formation will be observed.

5. The precipitate is then refluxed in a microwave oven for 60 min.

6. After refluxing the precipitate is washed to reduce the pH to 7.After this the gel is dried and ground to a fine powder.

7. The powder is calcined at a temperature of 1100^{o}C.

Table 3.1: calculated weight amount in grams for synthesis of samples through in-situ route.

(LSMO:NFO)	**Nickel chloride(g)**	**Ferric cloride(g)**	**Lanthanum acetate(g)**	**Stroncium chloride(g)**	**Manganeses acetate(g)**
50:50	3.6227	4.9441	3.2271	1.3408	3.7351
60:40	2.9167	3.98	3.896	1.6189	4.5096
80:20	1.4671	2.0016	7.799	2.1713	6.0488

3.3 Synthesis of LSMO: $NiFe_2O_4$ composites by solid-state route

3.3.1 Experimental Setup

The synthesized pure powders of LSMO and NFO are taken in the measured weights according to the table and a mixed and ground to a fine powder with the help of a mortar and pestle.

Table 3.2: calculated weight amount in g for synthesis of samples through solid state route.

LSMO:NFO	LSMO (g)	NFO (g)
80: 20	0.48	0.12
50: 50	0.3	0.3
60: 40	0.36	0.24

Preparation of pellets and sintering:-

1. To make a circular pellet 0.6 g of the power is take in a mortar pestle. Two drops of PVA binder is added and the powder is ground and pressed.
2. Sintering is done in a raising hearth furnace at a temperature of 1200 degrees and a hold time of 2 hrs.

3.4 General characterization

Thermal (DSC-TG)

The differential scanning calorimetry and thermogravimetric analysis was carried out in(NETZCH STA 449 C, Germany).The characterization were made with a heating rate of 10ºC/min in the temperature range 30 ºC to 1000 ºC.

Structural (XRD)

The XRD patterns were obtained from Phillips PANalytical (model number PW 3040,Netherland) diffractometer with a Cu Kα radiation (λ=0.15406 nm) with a graphite secondary beam monochromator; the intensities were obtained in a 2θ range between 20º and 80º; with a step rate of 0.04/sec(measuring time of 25mins).Debye-Scherer relation was used to determine the crystallite size.

Microstructural (SEM with EDAX)

The micro structural analysis were obtained from Scanning Electron Microscope (model-JEOL JSM 6480LV).The Secondary electron images were obtained to study the surface topology and backscattered electrons images the mass discrimination (contrast mechanism).Chemical analysis were obtained with the help of EDAX.

Density Measurement

The density and porosity measurement for the sintered pallets were obtained and shown in the following table. The bulk density was calculated using the formula B.D = $\frac{D}{W-S}$ * 0.81, and the apparent porosity using the formula A.P = $\frac{W-D}{W-S}$ * 100; where 0.81 refers to the value of the density the liquid used to carry out the experiment. In this case it was kerosene and whose density is 0.81 g/cm^3 .

Magnetic hysteresis loop

The PULSE FIELD HYSTERISIS LOOP TRACER of MAGNETA (MUMBAI) was used to trace the MH loop for sintered pellets of both compositions. It can measure a magnetic field of 0.5 Tesla. The machine was first calibrated using VSM data of standard NF having saturation magnetization of 72.4 emu/g.

The pellet of both compositions was then placed in the sample holder one by one in the machine so as to obtain their M-H loop.

The M-H loop can be used to obtain following data

Coercive Field (O_e)

Remanent magnetization (Mr) in emu/g

Saturation magnetization (M_s) in emu/g

Chapter 4

RESULTS AND DISCUSSIONS

4.1 Characterization of pure LSMO and $NiFe_2O_4$

4.1.1 Thermal

Figures 4.1.1 (a) and (b) shows the DSC-TG profiles of as-prepared LSMO and NFO powders, respectively.

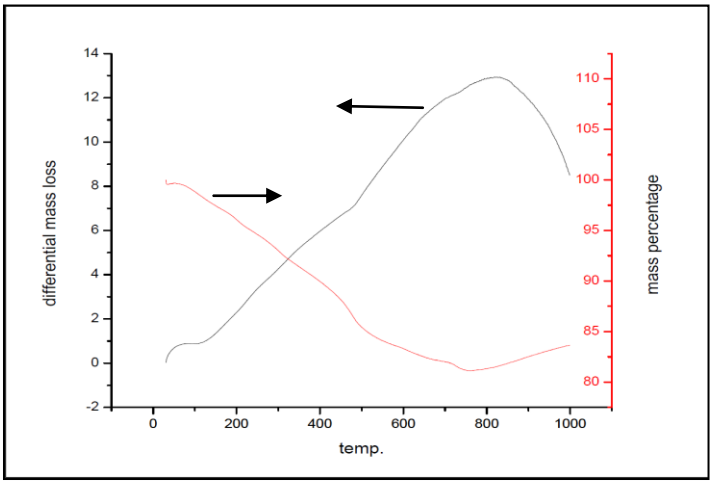

(a)

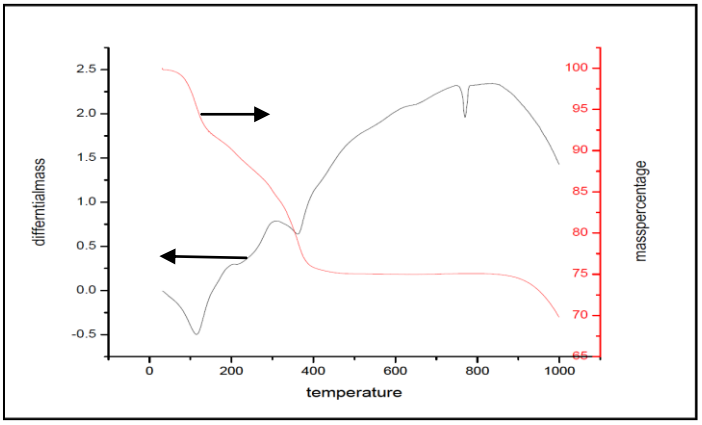

(b)

Fig 4.1.1: DSC-TG of as-prepared (a) LSMO and (b) NFO.

Two distinct regions (30-450 °C and 450-800 °C) of weight loss are observed for pure LSMO and weight gain was observed beyond 800 °C. Similar weight loss was also observed for pure

NFO sample. The weight loss was due to the removal of absorbed or adsorbed water present in the sample. In the DSC plot there are an endothermic peak at ~ 110 °C and ~ 400 °C for both samples. The broad exothermic peak starting from 600 °C to 1000 °C was observed in DSC plot for both samples and is probably due to the crystallization temperature of either LSMO or NFO.

4.1.2 Structure and microstructure

The presence of various phases and crystallite size were determined from the X-ray diffraction pattern. Figures 4.1.2 (a) and (b) shows the XRD patterns of LSMO and NFO samples sintered at 1200 ‘C.

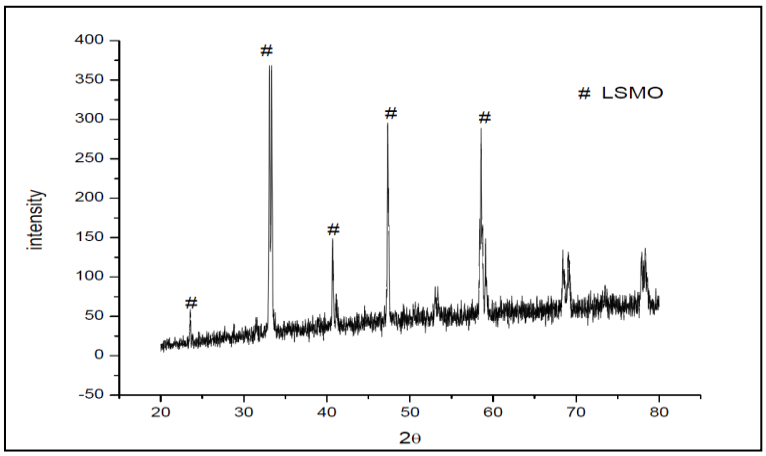

(a)

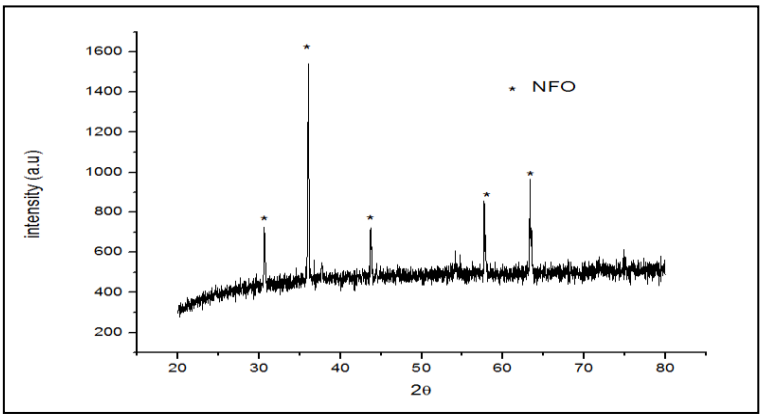

(b)

Fig 4.1.2: XRD patterns of (a) LSMO (b) NFO sintered at 1200 °C.

All the peaks are assigned to LSMO and NFO phase as confirmed from the JCPDS files (47-0444 For LSMO and 03-0875 for NFO). Structure of LSMO and NFO was rhombohedral and

cubic, respectively. The most intense peak of NFO comes (311) plane. The crystallite size of LSMO and NFO was found to be around 30 nm and 55 nm, respectively.

Scanning electron microscopy (SEM) gives the information about the size, shape and agglomeration behavior of sintered pellets. Figure 4.1.2 (c) and (d) shows the SE and BSE images of LSMO sintered samples.

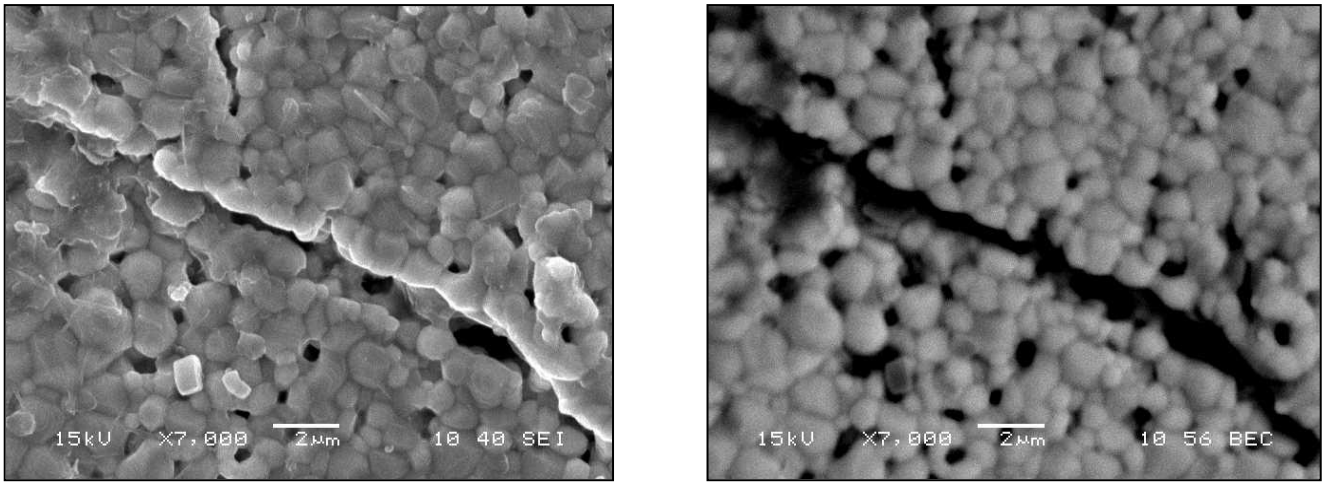

(c) (d)

Fig 4.1.2: (c) SE image of LSMO (d) BSE image of LSMO.

From the BSE-image, it can be seen that there is no secondary phase present and the crack propagation is mostly through grain boundary and the pores can be a reason for the propagation through grain boundary.

4.1.3 Density

The bulk density and apparent porosity of sintered LSMO pallets were obtained as 4.27 g/cc and 25 % respectively.

The bulk density and apparent porosity for sintered NFO pallets were obtained as 3.76 g/cc and 33 % respectively.

The bulk density and apparent porosity of LSMO and NFO samples are given in Table 4.4.

4.1.4 Magnetic hysteresis loop

M-H loop shows the magnetic behavior of a material at room temperature; provides the values for Coercive Field (O_e), Remanent magnetization (Mr) in emu/g, Saturation magnetization (M_s) in emu/g. Figure 4.1.4 (a) shows the M-H loop of pure NFO pallet ,which was sintered at 1200 °C.

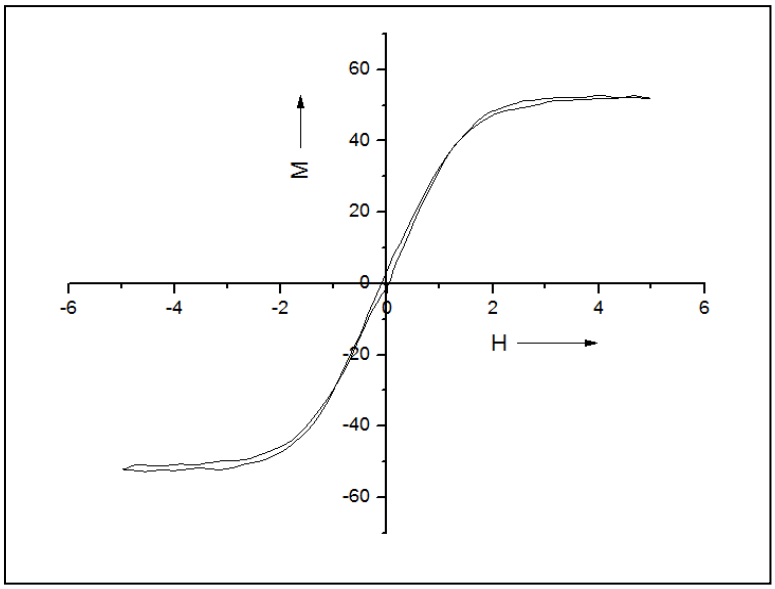

(a)

Fig 4.1.4: M-H curve (a) NFO.

From the M-H curve we can infer that the NFO sample prepared belongs to soft magnet and the saturation magnetization (Ms) and coercivity (Hc) value comes out to be 52.7 emu/g and ~74 Oe, respectively. The MH loop of pure LSMO could not be measured due to the low magnetization of LSMO at room temperature.

4.1.4 Remarks

Pure form of LSMO and NFO were successfully prepared through precipitation route using kitchen microwave oven. Crystallite size of LSMO (monoclinic) was found to be smaller than NFO (cubic). At room temperature, there is no magnetic behavior shown by LSMO, where as NFO has soft magnet behavior.

4.2 Characterization of in-situ LSMO: $NiFe_2O_4$ composites

4.2.1 Thermal

Figures 4.2.1 (a), (b) and (c) shows the DSC-TG profiles the composite of LSMO and NFO with ratios 50:50, 60:40 and 80:20 respectively; in-situ synthesized and sintered at 1200 ‘C for 2 hours.

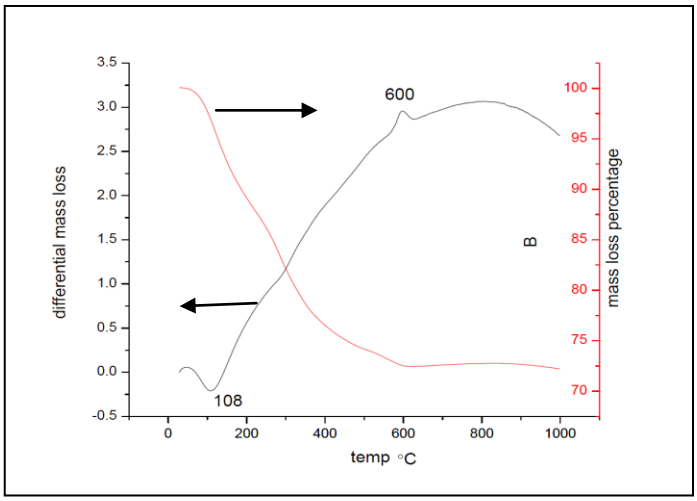

(a)

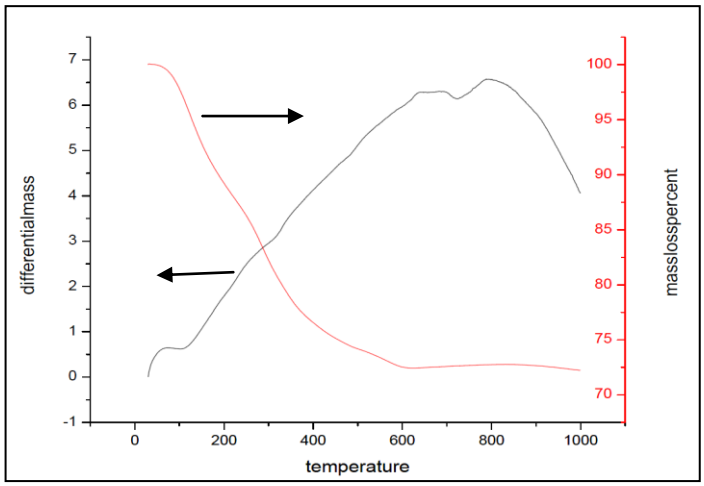

(b)

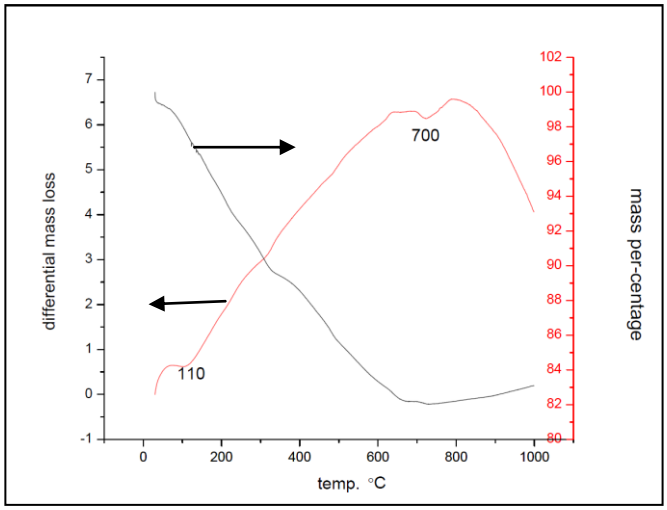

(c)

Fig 4.2.1: DSC-TG curve of (a) 50:50 (b) 60:40(c) 80:20 in-situ synthesized composites.

Two distinct regions (30-450 °C and 450-800 °C) of weight loss are observed for in-situ synthesized 50:50(LSMO: NFO), 60:40(LSMO: NFO), and 80:20(LSMO: NFO). The weight loss was due to the removal of absorbed or adsorbed water present in the sample. In the DSC plot, the broad exothermic peak starting from 600 °C to 1000 °C was observed in DSC plot for all samples and is probably due to the crystallization temperature of either LSMO or NFO.

4.2.2 Structure and microstructure

The presence of various phases and crystallite size were determined from the X-ray diffraction pattern. Figures 4.2.2 (a), (b) shows the XRD patterns of in-situ synthesized composites with composition50:50(LSMO: NFO) and 80:20(LSMO: NFO) respectively. All the peaks are. identified either LSMO or NFO with the help of JCPDS without any impurities.

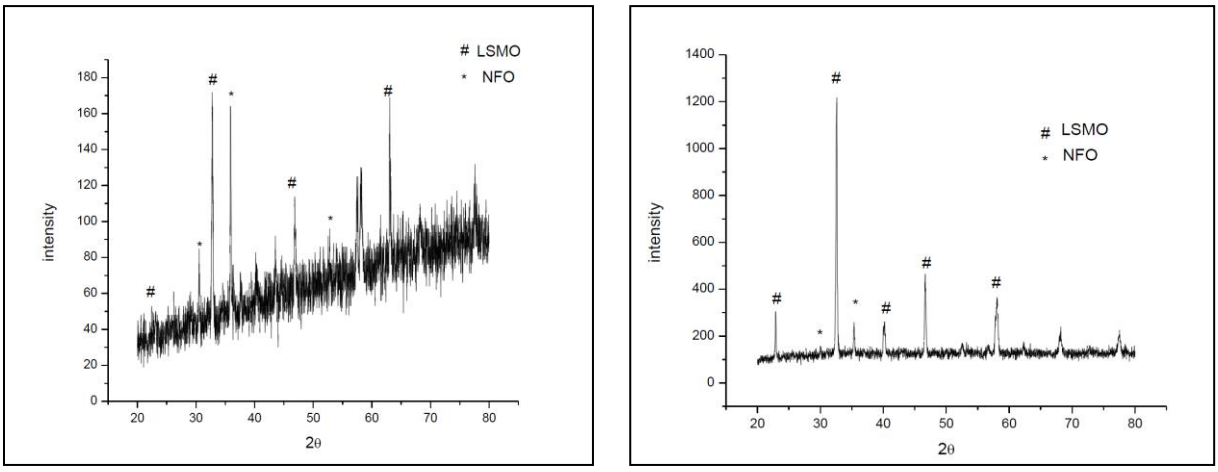

(a) (b)

Fig 4.2.2: XRD pattern of (a) 50:50, (b) 80:20; SEM images of (c) SE image of 80:20(d) BSE image of 80:20

Figures 4.2.2 (c), (d) shows the secondary electron image and backscattered image of in-situ synthesized 80:20(LSMO: NFO) composite.

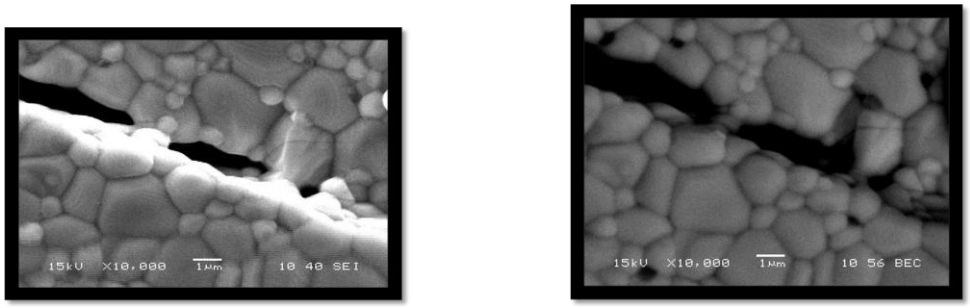

(c) (d)

Figures 4.2.2 (c), (d) shows the secondary electron image and backscattered image of in-situ synthesized 80:20(LSMO: NFO) composite

Figure 4.2.2 (e), (f) shows the secondary electron image and backscattered image of in-situ synthesized 80:20(LSMO: NFO) composite and their respective EDAX

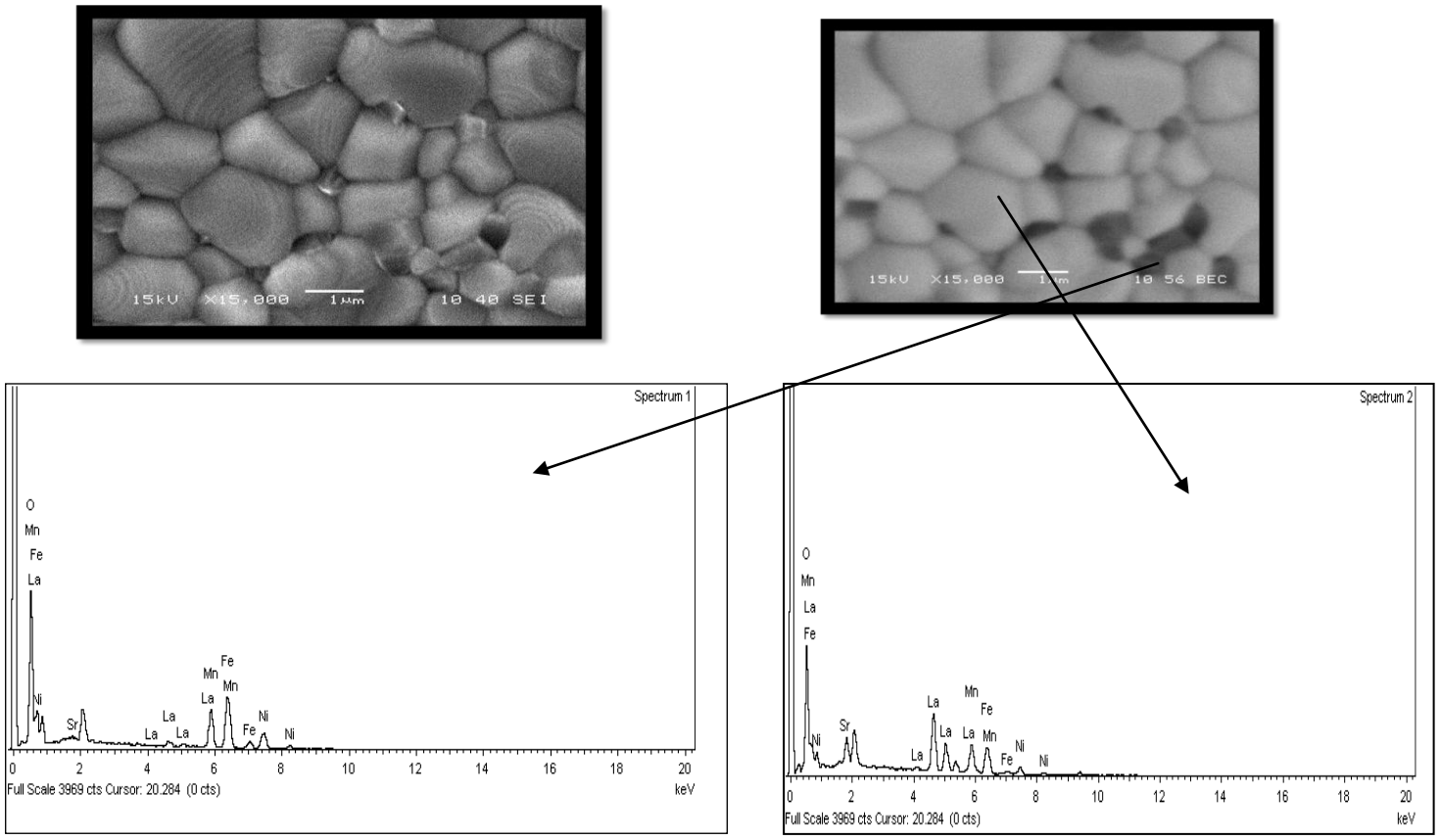

Fig 4.2.2: (e) SE image of 80:20 (f) BSE image of 80:20 with EDAX

The Fig 4.2.2 (c), (d) shows the crack propagation in the sample, the crack propagation is mainly through the grain boundary and there are some micro-cracks passing through the grains. The Fig 4.2.2 (e), (f) shows the compactness of the material, as well as we can infer that the grain size of NFO is much smaller than the grain size of LSMO. From the BSE image the part with dark contrast was found out to be NFO and the part with bright contrast to be LSMO with the help of EDAX.

4.2.3 Density

Table 4.1 shows the bulk density and apparent porosity of in-situ synthesized composites, those are sintered at 1200 ºC.

Table 4.1: Bulk density and apparent porosity of the in-situ prepared samples.

Serial No.	Sample (LSMO:NFO)	Bulk density(g/cc)	Apparent porosity(percentage)
1	50:50(IS*)	4.52	25
2	60:40(IS)	5.01	20
3	80:20(IS)	5.44	17

4.2.4 Magnetic hysteresis loop

Figure 4.2.3 (a),(b),(c) shows the hysteresis loop of in-situ synthesized composite at temperature 1200 ºC of composition 50:50(LSMO: NFO),60:40,80:20 respectively.

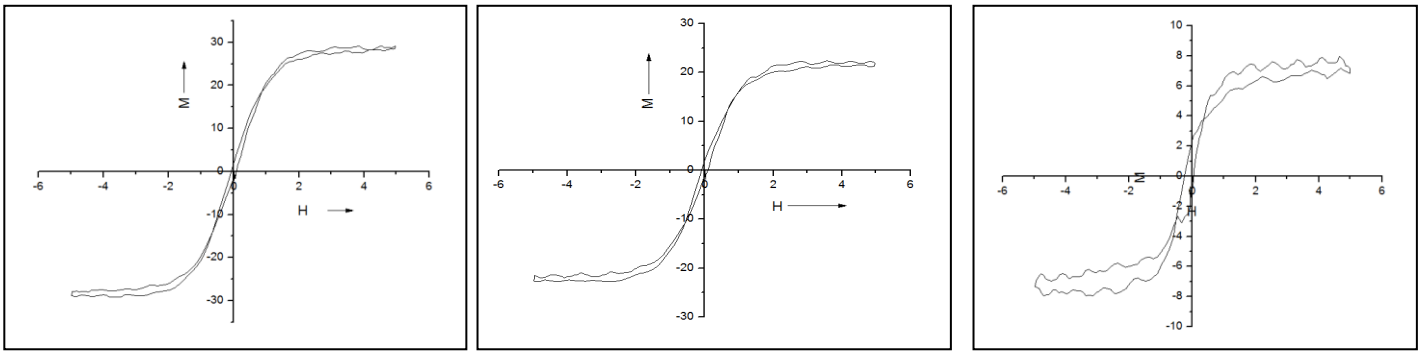

(a) (b) (c)

Fig 4.2.3: MH loops (a) 50 LSMO: 50 NFO, (b) 60 LSMO: 40 NFO, and (d) 80 LSMO: 20 NFO samples

As we are increasing the percentage of LSMO the magnetic behavior (hysteresis) keeps deteriorating. This mainly because of the increase in the percentage of LSMO, as LSMO does not show any magnetic behavior at room temperature, this discrepancy in the hysteresis loop can be seen. The saturation magnetization, coercivity is given in Table 4.5.

4.2.4 Remarks

From the DSC-TG graphs of the in-situ composition shows the calcined temperature for the samples, which is around 800-1000 ^{o}C. In-situ prepared samples show a great deal of compactness as seen from the SEM images, which certainly can help in increasing the magnetic property of the samples. As we are increasing the ratio of LSMO we can study a variation in the magnetic behavior. The amount of distortion in the M-H loop keeps on increasing as we keep on increasing the percentage LSMO. So we can prepare sample as per the requirement of a material by deciding the ratio of LSMO: NFO.

4.3 Characterization of LSMO: $NiFe_2O_4$ composites by solid-state route

4.3.1 Structure and microstructure

Figures 4.3.1 (a), (b), (c) shows the XRD patterns of solid route synthesized composites with composition 50:50(LSMO: NFO), 60:40 (LSMO: NFO) and 80:20 (LSMO: NFO) respectively. All the peaks are identified either LSMO or NFO with the help of JCPDS without any impurities.

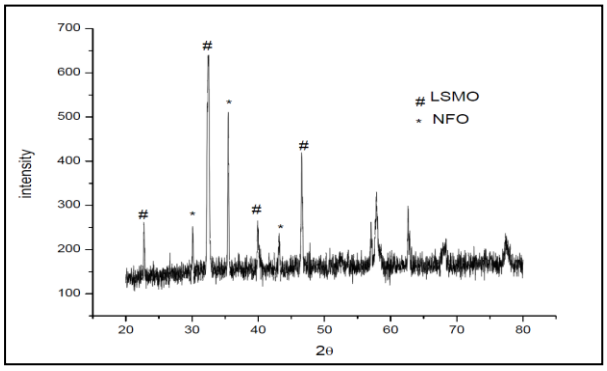

(a)

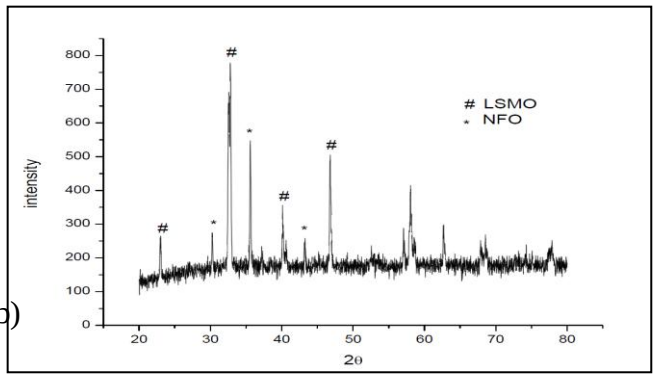

(b)

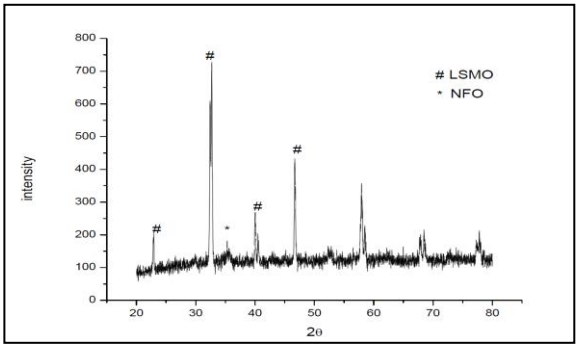

(c)

Fig 4.3.1: XRD pattern of (a) 50 LSMO: 50NFO, (b) 60 LSMO: 40 NFO and (c) 80 LSMO: 20 NFO

Figures 4.3.1 (d), (e) shows the secondary electron image and backscattered image of solid route synthesized 80:20(LSMO: NFO) composites.

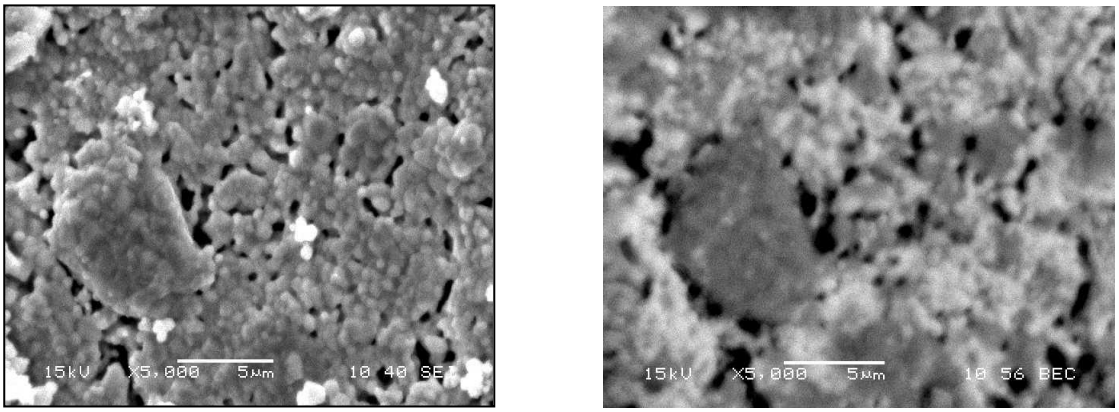

(d) **(e)**

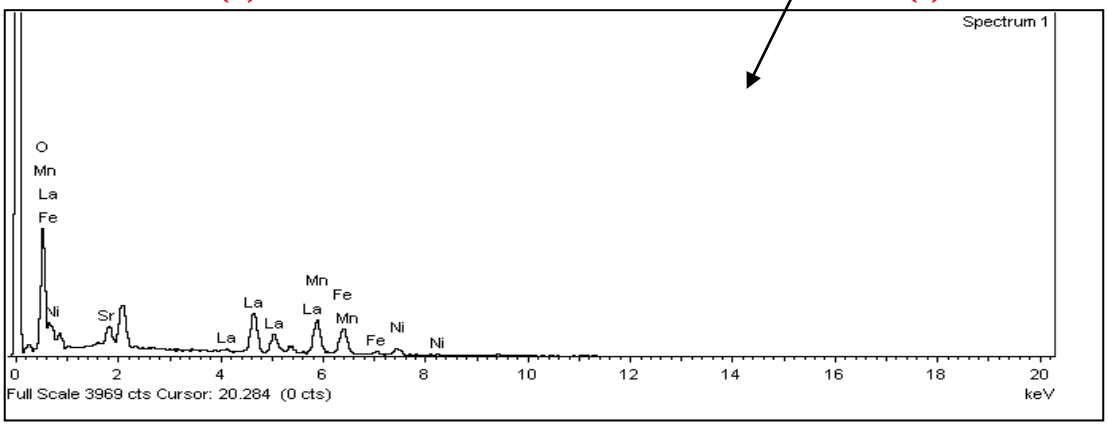

Fig4.3.1: SEM image of (d) 60:40(Secondary Electron image), (e) 60:40 (backscattered electron image) showing EDAX.

The table 4.2 shows the composition ratios of the 60:40 (LSMO: NFO) sample, the values were taken with help of EDAX.

Table 4. 2: whole surface EDAX of 60:40 (LSMO: NFO) sample.

Element	App Conc.	Intensity Corrn.	Weight%
O K	22.47	1.7320	21.76
Mn K	9.53	0.9470	16.68
Fe K	9.54	0.9712	16.28
Ni K	3.81	0.9742	6.47
Sr L	2.59	0.6930	6.18
La L	18.81	0.9553	32.63
Total			100

The crystallite size of LSMO and NF was found to be around 45 nm and 70 nm, respectively. The Fig 4.3.1 (c), (d) shows the tropography of solid route synthesized sample, the image shows that the porosity level in this sample are much more than in-situ route prepared sample. The BSE image shows the presence of two phases in the sample and it can be seen from the EDAX of whole surface. From the above table the ratio of LSMO and NFO comes out to be 66.37 LSMO: 33.63 NFO.

4.3.2 Density

Table 4.3 shows the bulk density and apparent porosity of in-situ synthesized composites, those are sintered at 1200 ºC.

Table 4. 3: Bulk density and apparent porosity of solid route synthesized samples

Serial No.	Sample (LSMO:NFO)	Bulk density(g/cc)	Apparent porosity(percentage)
1	80:20(SS*)	5.43	15
2	60:40(SS)	5.03	18
3	50:50(SS)	4.70	21

Table 4.4 shows the bulk density and apparent porosity of different synthesized sample, with different composition and different routes.

Table 4. 4: Bulk density and apparent porosity synthesized samples

Serial No.	Sample (LSMO:NFO)	Dry weight (D) gms	Soaked weight (W)gms	Suspended Weight (S)gms	Bulk density(g/cc)	Apparent porosity($\frac{W-D}{W-S}$) (percentage)
1	80:20(SS*)	0.6076	0.6212	0.5306	5.43	15
2	60:40(SS)	0.6034	0.6206	0.5236	5.03	18
3	50:50(SS)	0.6447	0.6684	0.5573	4.70	21
4	50:50(IS*)	0.6209	0.6488	0.5377	4.52	25
5	60:40(IS)	0.5770	0.5961	0.5027	5.01	20
6	80:20(IS)	0.6309	0.6467	0.5528	5.44	17
7	NFO(IS)	0.6023	0.6449	0.5150	3.76	33
8	LSMO(IS)	0.5233	0.5485	0.4492	4.27	25

SS*=solid state route, IS*=in-situ route

4.3.3 Magnetic hysteresis loop

Figure 4.3.2 (a), (b) and (c) shows the hysteresis loop of solid route synthesized composites at temperature 1200 ºC of composition 50:50(LSMO: NFO), 60:40, 80:20 respectively.

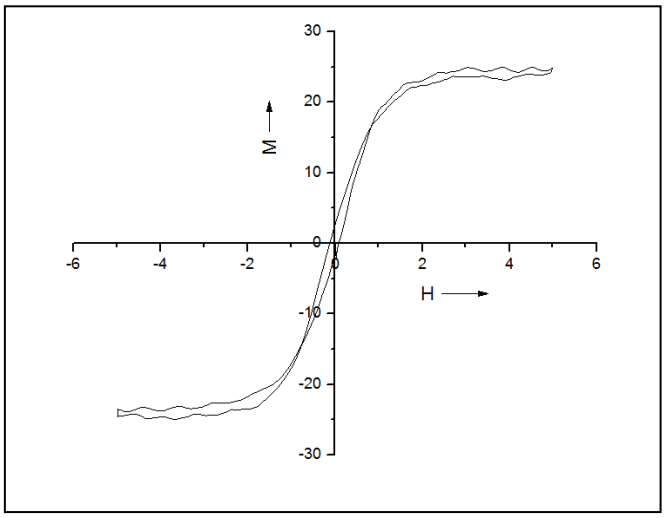

(a)

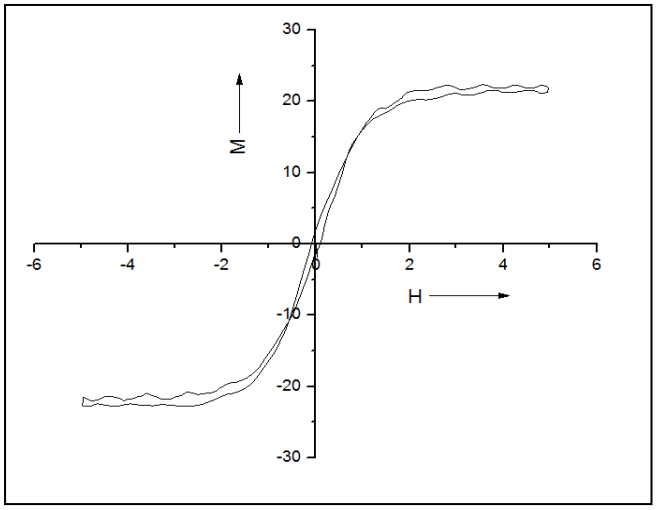

(b)

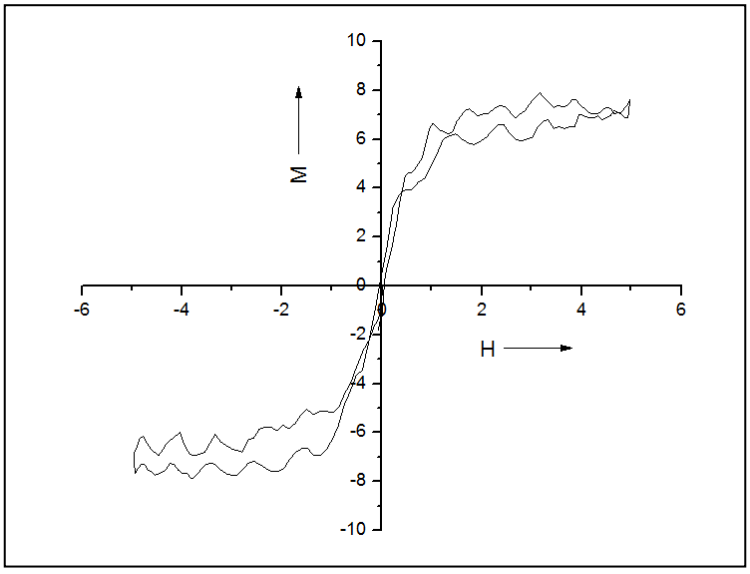

(c)

Fig 4.3.2: Magnetic Hysteresis loop (a) 50:50, (b) 60:40, and (d) 80:20

The behaviors shown by solid route synthesized are almost similar to that of in-situ synthesized samples. The change in the hysteresis loop can be seen as we keep on increasing the percentage of LSMO present in the sample and decreasing the percentage of NFO. The magnetic property keeps deteriorating at room temperature as we are increasing the percentage of LSMO.

Table 4.5: shows the values for Coercive Field (O_e), Remanent magnetization (Mr) in emu/g, Saturation magnetization (M_s) in emu/g in different composition of LSMO and NFO, prepared by different routes.

Composition	Process	Ms(emu/g)	Mr(emu/g)	Hc
NFO	In-situ	52.7	0.5439	73.4
LSMO	In-situ	****	****	****
50:50	Solid-solid	25	2.3675	102.53
50:50	In-situ	29.17	0.225	58.50
80:20	Solid-solid	7.90	3.033	36.11
80:20	In-situ	7.90	0.0072	110
60:40	Solid-solid	22.34	-0.552	59.45
60:40	In-situ	22.80	0.77	70.03

4.3.4 Remarks

The solid state despite of being simple way to prepare a composition it has its discrepancies. The samples those were prepared have higher porosity compared to that of in-situ synthesized samples. The grain size and the proper distribution of the phase does depend on the amount of missing and grinding with mortar pestle, so the grain properties can be improved by increasing the amount of grinding.

Chapter 5

CONCLUSIONS

The findings of the present work are summarized below:

1. The effect of route followed for the synthesis of the sample plays a vital role in the compactness and magnetic behavior of the sample. The compactness is much higher in in-situ route compared to solid state route. The variation in porosity can be seen from the SEM images of in-situ and solid route samples.
2. The sample preparation through co precipitation method, the state where we get the gelation should be taken into account; it is after this state only the precipitation starts. So the KOH with ethylene glycol was added till we get a gelation state.
3. The percentage of LSMO plays a vital role with magnetic behavior of the sample. As we are increasing the percentage of LSMO in the composition we can see an increase in distortion at the room temperature. As per the requirement of the material the percentage of LSMO can be maintained to get the desired result.
4. Cracks were impregnated for the study of the behavior of crack propagation; which seems to be mostly through the grain boundaries and some micro cracks are formed through the grains.
5. The NFO phase was found to be in the grain boundaries or grain junctions; at the corner of two or three grain junction .This was the result in the decrease in the magnetic behavior of the sample. In the composite with low percentage of NFO phase, and the NFO phase being in the edge of LSMO grains increases the distortion in the hysteresis loop.
6. The size of NFO grains is much smaller than the size of LSMO grains.

REFERENCES:

1. T. Tang, S. Y. Zhang, R. S. Huang, and Y. W. Du, *J. Alloys and Comp.*, **353**, (2003) 91.
2. B.B. Nayak, S. Vitta, A.K. Nigam, D. Bahadur, Mater. Sci. Eng. B **113** (2004) 50.
3. Q. Huang, J. Li, X. Huang, C. K. Ong, and X. S. Gao, *J. Appl. Phys.*, **90** (2001) 2924.
4. C.-H. Yan, Z.-G. Xu, T. Zhu, Z.-M. Wang, F.-X. Cheng, Y.-H. Huang, and C.-S. Liao, *J. Appl. Phys.*, **87** (2000) 5588.
5. C. Zener, *Phys. Rev.*, **82** (1951) 403.
6. M. W. Barsoum, "Fundamentals of Ceramics", IOP publishing, Bristol and Philadelphia, 2003 page-530.
7. K.P. Lim, K.P. Lim, S.W. Ng, S.A. Halim, S.K. Chen and J.K. Wong, J. Applied Sci., **6** (2009) 1153-1157.
8. Carter, C. Barry ;Norton,M.Grant "Ceramic materials:science and engineering" springer, 2007.ISBN 0387462708
9. Shriver,D. F.;Atkins,P . W.; Overton, T. L;Rouke,J. P.; Weller, M. T.; Armstrong,F . A. "Inorganic Chemistry" W. H. Freeman, New York, 2006. ISBN 0-7167-4878-9.
10. Mishra,S.;Karak, N.;Kundu,T. K. ;Das,D.;Maity, N., Chkravorty, *Material Letters*,**60,1111**(2006)
11. Murdock,E. S.;Simmsons, R . F.;Davidson, R.; *IEEE Trans. Magn.* **28, 3078**(1992).
12. Kim W.C.;Kim,S.J,Lee. S. W.;Kim C.S.;*Magn. Mater*. **226,1418**(2001)
13. Kharabe, R.G.; Devan, R.S.; Kanamadi, C.M.; Chougule, B.K; *Smart Mter.* **15, N36** (2006).
14. Satyanarayana, L.; Madhusudan Reddy, K. ; Manorama, S.V.;*Mater. Chem. Phys*. **82, 21**(2003).
15. Rana, S.; Gall, A. ; Srivastava, R.S.; Misra, R.D.K. ; *Acta Biomaterialia* **3,233**(2007).
16. Singhal, S.; Chandra, K. ; *J. Solid State Chemistry* **180,296**(2007).
17. Smit, J.; Wijin, H.P.J.; *Ferrites* (Philips technical Library, Netherlands, 1959).
18. Giannakopoulou, T.; Kompotiatis, L.; konogeorgakos, A.; Kordas, G.; *J. Magn. Magn. Mater.* **246,360**(2002).
19. Y. Mortimo ans A. Asamitsu, Kuwahara H. and Tokura, Y. ; *Giant magnetoresistance of manganese oxides with a layered perovskite structure,Nature* **380,141** (1996).